Solution behaviour of semiflexible polyelectrolytes with anisotropic counterions

Can Hou,[1] Max Hohenschutz,[1] Takaichi Watanabe,[2] Walter Richtering,[1,3] and Carlos G. Lopez[4]
[1)] *Institute of Physical Chemistry, RWTH Aachen University, Landoltweg 2, 52056 Aachen, Germany, European Union*
[2)] *Department of Applied Chemistry, Graduate School of Natural Science, Okayama University, 3-1-1, Tsushima-naka, Kita-ku, Okayama 700-8530, Japan*
[3)] *DWI - Leibniz-Institut fur Interaktive Materialien, RWTH Aachen University, Forckenbeckstraße 50, 52074 Aachen, Germany, European Union*
[4)] *Department of Materials Science and Engineering, The Pennsylvania State University, 1 Pollock Rd, State College, 16802, US*

(*Electronic mail: cvg5719@psu.edu)

(*Electronic mail: richtering@rwth-aachen.de)

We investigate the solubility, structure, and electrical conductivity of aqueous solutions of the semiflexible polyelectrolyte carboxymethyl cellulose (CMC) with two types of divalent counterions: small symmetric metal ions and organic anisotropic ions in which the charges are located near the ends of the molecule. Conductivity measurements show that, at high concentrations, the anisotropic counterions dissociate from the polymer to a greater extent than the small metal ions. At lower concentrations, the fraction of dissociated counterions is similar for both systems. These differences in dissociation are reflected in the scattering patterns: solutions containing anisotropic counterions display a clear correlation peak, consistent with higher local order, whereas those with divalent metal ions show only a broad correlation shoulder, indicating weaker spatial correlations. The stretching parameter obtained from SAXS measurements correlates positively with the effective charge of the chains obtained from electrical conductivity, in qualitative agreement with scaling theory. Our results demonstrate that counterion charge topology provides a tunable parameter for controlling polyelectrolyte conformation and solution thermodynamics.

I. INTRODUCTION

The properties of polyelectrolyte solutions depend on the nature of the counterions neutralising the polymer backbone.[1] For example, divalent counterions condense onto the backbone at approximately twice the rate as monovalent ones,[2–4] leading to lower effective backbone charges. This results in lower osmotic pressure and reduced chain dimensions.[5–9] Counterion-solvent interactions can also be used to tune the phase behaviour,[1,10,11] charge transport[12,13] and interfacial[14] properties of polyelectrolyte solutions and gels. Understanding how counterion properties govern polyelectrolyte solution behaviour is therefore essential for designing charged polymers with targeted properties.

The finite size of ions sets a minimum distance of closest approach, which influences the spatial distribution of counterions around the polymer backbone. Based on this, Oosawa[15] predicts that larger counterions exhibit a higher degree of dissociation than smaller ones. More significant than the excluded volume from the bare ion radius is the presence of hydration shells,[16–25] which govern ion pairing and have been proposed to determine properties such as ion selectivity in polyelectrolyte solutions and gels.[26,27]

For monovalent counterions, experiments show that despite substantial differences in solvation shell structure,[29?] alkali metal and tetraalkylammonium salts of anionic polyelectrolytes exhibit only small differences in the fraction of dissociated counterions. An example is shown in figure 1, which plots the electrical conductivity of various polystyrene sulfonate (PSS) salts as a function of concentration, together with the fraction of charged monomers inferred from the conductivity data from Szymczak et al.[12] The differences among the monovalent salts are at most about $\simeq 10\%$.

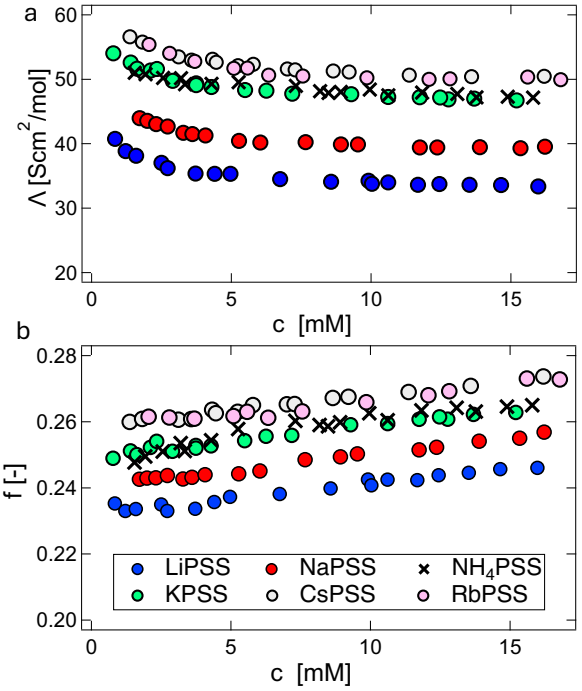

FIG. 1. a: conductance of PSS solutions, data from [12]. b: fraction of monomers with a free counterion calculated with the model of Colby et al.[28] using $\xi[\text{Å}] = 33c^{-1/2}$ for all salts, where c is in units of moles of repeating units per dm^3.

Recently, we have studied the properties of the semiflexible polyelectrolyte carboxymethyl cellulose (CMC) as a function of counterion type. Large, hydrophobic counterions promote solubility in non-aqueous media,[11] whereas the viscosity, scattering, and thermodynamic properties of different monovalent salts of CMC in water are largely independent of ion identity.[3,30,31] A similar insensitivity to ion type has been reported for alkaline earth salts of CMC, where the osmotic coefficient remains approximately constant across different cations,[32,33] in line with experimental reports for other polysaccharides.[34–36] One notable exception arises at high concentrations, where CMC with hydrophobic counterions exhibits a decoupling of polymer and counterion concentration fluctuations. An example of this behaviour is shown in figure 2. Such a behaviour is not observed for hydrophilic counterions such as alkaline metals.[37] These results suggest that counterion-solvent interactions influence the spatial distribution of free counterions around the polymer backbone. However, the fraction of free counterions, as evaluated from conductivity, is largely insensitive to counterion-solvent interactions.[31]

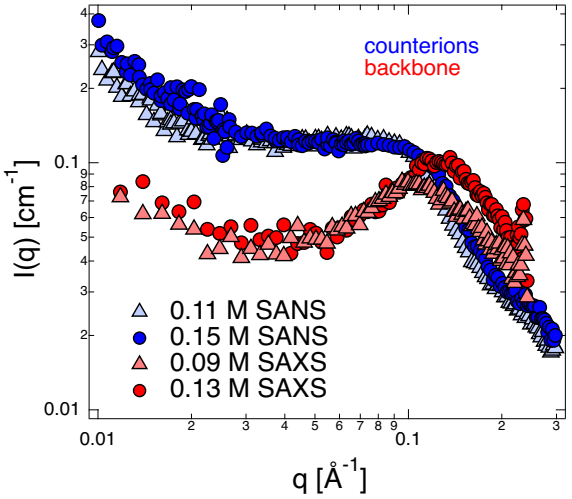

FIG. 2. SANS and SAXS intensities of tetrabutylammonium carboxymethylcellulose (TBACMC) solutions in DI water or D_2O without added salt. In SANS, the scattering signal is dominated by the contribution from the counterions and in SAXS from the polymer backbone. SANS data are in absolute units of cm^{-1} and SAXS data are in arbitrary units shifted to match the SANS data for clarity. Note that counterions appear to be less strongly correlated (more de-localised) than the polymer chains. Data from ref. [37].

Earlier simulation studies have investigated the effect of counterion-solvent affinity[38–40] and counterion size.[41,42] The influence of counterion shape and charge distribution for multivalent counterions has been studied theoretically and by simulations for charged planar surfaces and cylindrical polyions.[43–48] Depending on the separation between charges and coupling parameter ($u = l_B/b$, where l_B is the Bjerrum length and b the distance between charges), anisotropic counterions can generate attractive forces between planar surface through bridging interactions. These effects are relevant to biological systems such as DNA condensation by stiff polyamines, including spermidine and spermine,[45,47] and antibody-mediated binding of charged lipid membranes.[44] For cylindrical polyions, Cha et al[48] find that divalent, rod-like counterions with charges placed at the end of the rods, behave as two monovalent counterions when the distance between charges is smaller than the distance from the polyion and as point-like divalent ions when the distance to the polyion is much larger than the separation between charges.

Anisotropic multivalent counterions represent an interesting class of ions. Unlike divalent metal ions, where the charge is localized at a single center, organic anisotropic counterions can be ditopic, with two unit charges located near the ends of the ion rather than concentrated at a single point. Two examples of such ditopic counterions, hexamethonium and suxamethonium, are shown in figure 3. Hexamethonium-containing compounds were once used for the treatment of hypertension.[49–51] Hexamethonium is a ganglionic blocker that competitively binds to nicotinic receptors in neuronal cells and inhibits sodium ion transport.[52,53] Although it has been discontinued as a therapeutic agent, it is still used in research, for example as a structure-directing agent in zeolite synthesis,[54–56] in complexes with fullerene molecules for enhanced drug delivery,[57,58] and in studies of its biological effects as an inhibitor.[59–61]

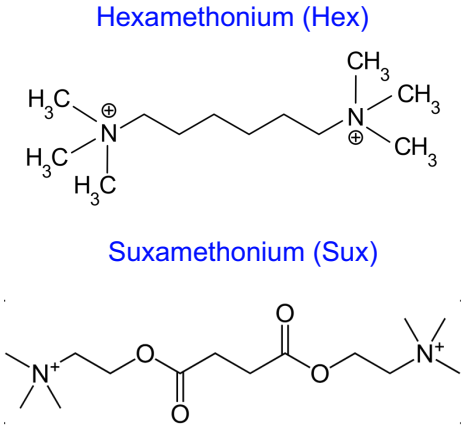

FIG. 3. Structure of the two ditopic counterions used in this study: hexamethonium (Hex) and suxamethonium (Sux).

In this study, we compare the scattering and electrical conductivity of carboxymethyl cellulose with hexamethonium and suxamethonium (or succinylcholine) counterions to those of CMC with conventional monoatomic counterions, including alkali and alkaline earth metal ions. The observed differences are explained in terms of the fraction of free counterions, which is larger for ditopic counterions relative to monotopic ones such as Mg^{2+}. Our results show that charge topology can be used as a design variable to tune polyelectrolyte solution properties.

II. MATERIALS AND METHODS

Preparation of CMC salts: Hexamethonium bromide ($HexBr_2$) (Sigma Aldrich) was added to approximately 0.2M sodium carboxymethyl cellulose (NaCMC) aqueous solution, with a molar ratio of $HexBr_2$ to NaCMC monomers of more than 10:1. The NaCMC used was from the same batch used in [62], with the degree of substitution estimated to be 0.98 and a molar mass of 360 kg/mol, determined by static light scattering.[62] After the mixture is thoroughly dissolved and homogeneous, it was dialysed against DI water using membranes with MWCO = 12-14 kD obtained from SpectraPor. The de-ionised water used for the dialysis was obtained from an Abactus[2] Ultra Pure Water System (MembraPure Gmbh). The filled dialysis membrane is sealed and submerged in the deionised (DI) water, with the water periodically replaced until the conductivity reaches approximately 10^{-4} Sm^{-1}, which corresponds roughly to the conductivity of fresh de-ionised water. The same procedure was carried out for the ion exchange of NaCMC into metal salts using calcium bromide dihydrate (Sigma Aldrich), Cobalt Nitrate (Puriss p.a. ACS Reagent, $\geq$ 99.0%, Sigma Aldrich) or Zinc chloride (Zinc chloride, ultra dry, 99.99% metal basis) as the excess salt. Addition of a large excess of divalent metal ions led to precipitation of CMC. The entire mixture, including both precipitate and supernatant, was transferred to the dialysis bag. As the dialysis proceeds, the precipitate re-dissolves.[63] Succinylcholine dichloride of >99% purity was used for ion exchange to produce SuxCMC, and was also obtained from Sigma Aldrich. After dialysis, the polymers were freeze dried and solutions were prepared gravimetrically. To check that counterion exchange was complete with the above procedure, the HexCMC salt was dissolved in DI water, a 10-fold excess $HexBr_2$ was added followed by dialysis against DI water. The conductivity properties of the twice-exchanged and the single exchanged HexCMC were found to be identical.

Hansen solubility parameter (HSP) phase mapping: The experimental set-up for phase mapping was described in our previous work.[11] In essence, approximately 1 wt.% of the polymer was placed and sealed in a 5 mL transparent glass vial with an organic solvent or solvent mixture. The mixture was left for approximately 48 hours, after which the solubility status was recorded:

- ***Soluble:*** the solution is fully transparent and homogeneous, with no lumps or fragments visible.
- ***Insoluble:*** the initial piece of polymer placed remains mostly intact; no changes in the colour or opacity are observed.
- ***Partially soluble:*** there is a noticeable lump in the solution, or the solution is turbid but otherwise well mixed.

All non-aqueous solvents were obtained from Sigma Aldrich. The purity of all non-aqueous solvents used are listed in a table in the SI.

Synchrotron Small-angle X-ray Scattering (SAXS): SAXS measurements on CMC with anisotropic counter-ions were conducted at Beamline BL40B2 at SPring-8, Sayo, Japan. The temperature was set to be 25 °C, which was maintained by a Peltier heating unit. Acquisition times were set to 1 minute. The beam energy was 12.4 keV. The sample-to-detector distance was set to 1 m or 2m. For each sample, the scattering and transmission were recorded simultaneously. The scattering intensity was radially averaged and the intensity from the capillary was subtracted using standard reduction procedures. The SAXS data are reported in arbitrary units.

In-house Small Angle X-ray Scattering (SAXS): SAXS measurements on CMC with symmetric metal ions were performed on a 3-pinhole S-Max3000 system with a MicroMax002+ X-ray microfocus generator from Rigaku. Samples were irradiated with Cu K_α radiation (λ = 0.154 nm). The scattered beam was recorded using a two-dimensional multiwire detector (Gabriel design, 2D-200X with an active diameter of 200 mm) placed at a sample-distance of 2.6 m. A q-range of 0.05 to 4 nm^{-1} was covered with an off-center detection. Sealed 1.5 mm borosilicate capillaries from WJM Glas Müller GmbH served as sample containers. The magnitude of the scattering vector q was calibrated using Silver Behenate. The scattered intensity was corrected for dark noise, sample transmission and capillary thickness and was brought to absolute scale using a polyethylene standard.

Small-Angle Neutron Scattering (SANS): SANS measurements were performed on the LOQ beamline (ISIS neutron source, Didcot, UK) operating in time-of-flight mode with a white beam with wavelength range of 2.7–10.5 Å. The sample-to-detector distance was 4 m and the beam size 8 mm. Samples were loaded into cylindrical quartz cells of 2 mm pathlength and the data were reduced and solvent subtracted using standard procedures.

Electrical Conductivity: A SevenMulti Dual pH/conductivity meter (Mettler Toledo) was used for the conductivity measurements. The probe used was Cond Sensor InLab 710 (Mettler Toledo). The measurements were done at 25 °C, with the temperature controlled by placing the sample container in a temperature-controlled water bath. The conductivity probe was inserted into 10 mL polypropylene vials filled with approximately 4 mL of sample solutions, with the temperature sensor fully submerged. Readings were taken when the apparent temperature as shown by the conductivity meter agrees with that read on the water bath.

Density measurements: An Anton Paar DMA 5000 density meter was used to measure the density of CMC salts as a function of concentration. Results are reported in the supporting information.

Residual water content estimate: After dialysis and freeze-drying, the CMCs were exposed to air for approximately 24 h, after which approximately 15-30mg were loaded into a Simultaneous Thermal Analyzer (STA) 6000 (PerkinElmer), heated to 120 °C, and then held for at least 20 min. The difference of the final mass relative to the initial mass was recorded for each polymer and used to estimate the water content.

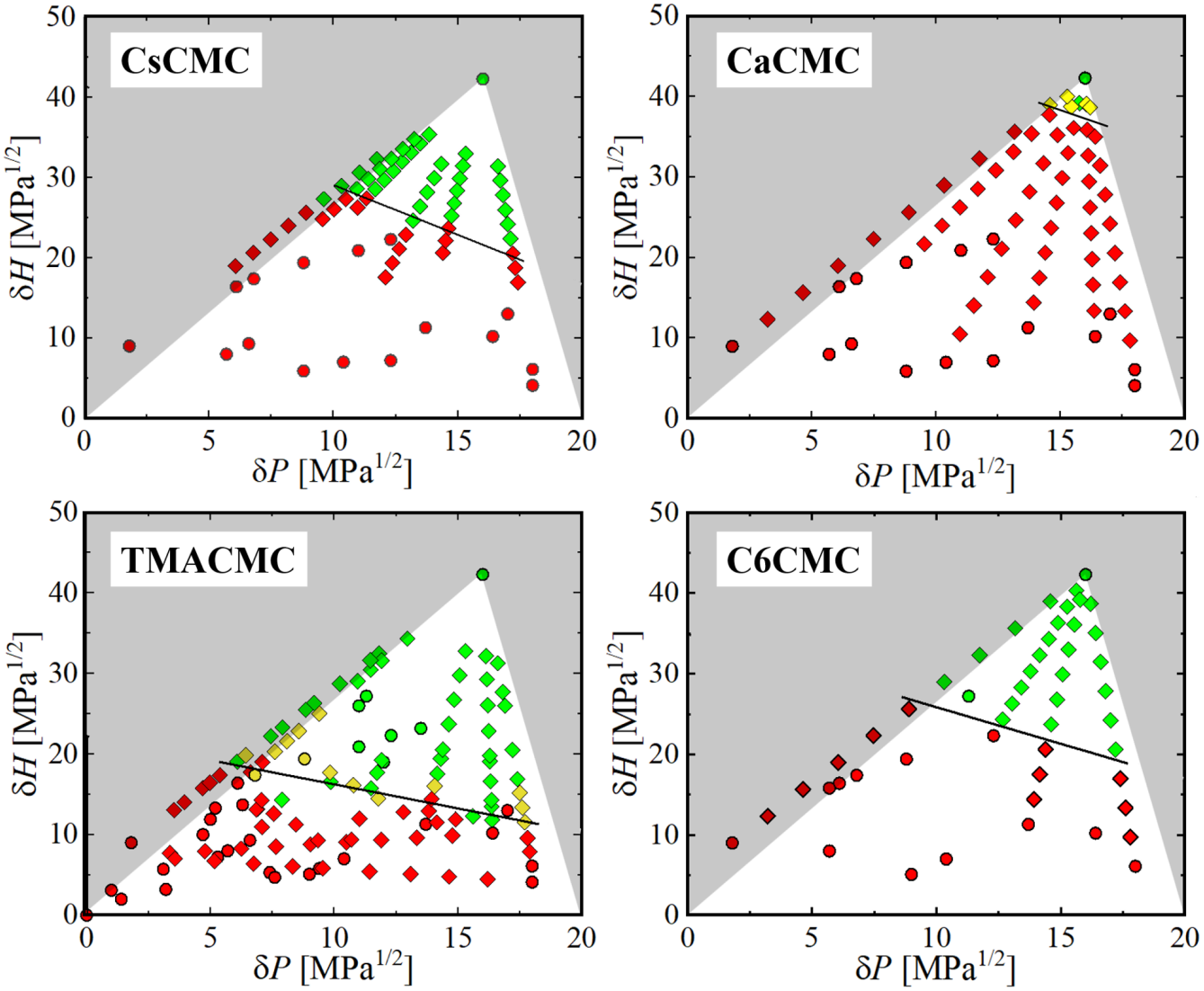

FIG. 4. Hansen solubility phase maps of mono- (Cs, TMA) and di-valent (Ca, Hex = hexamethonium) salts of CMC. The x-axis is the Hansen polarity parameter and the y-axis is Hansen's hydrogen bonding parameter. Circles are for pure solvents and diamonds are for mixed solvents. All solvents and solvent mixtures do not contain any added salt. Green symbols indicate soluble systems, red insoluble and yellow symbols are partially soluble, as described in section II. Black lines separate the soluble and insoluble regions, the method for establishing the solubility boundary is described in ref. 11. Data for CsCMC and TMACMC are from ref. 11. The solubility plot for SuxCMC is included in the supporting information.

III. RESULTS AND DISCUSSION

A. Solubility

Figure 4 plots the solubility maps of monovalent and divalent salts of CMC in the Hansen representation: δ_P represents the contribution of dipole interactions to the cohesive energy of a liquid and δ_H those of hydrogen bonding. The contribution of dispersion forces is not considered, following our earlier finding that the Hansen dispersion parameter (δ_P) does not correlate with polyelectrolyte solubility.[11] For all salts, it is observed that the polar, protic solvents such as water dissolve the polymer but apolar, aprotic solvents do not, in agreement with earlier results for various monovalent salts of CMC.[11]

The black lines in figure 4 designate the boundaries between the soluble and insoluble regions in Hansen space. For all systems studied, the boundaries are relatively sharp, demonstrating that δ_P and δ_H are useful parameters to predict the solubility of the various salts in single solvents and mixed solvent media.

Increasing the valence of the counterion leads to a decrease in the soluble region in the Hansen plots. This is expected because as the fraction of dissociated counterions decreases, the entropic gain for dissolution becomes weaker. Increasing the counterion hydrophobicity at fixed valence (i.e., going from Na^+ to TMA^+ or from Ca^{2+} to Hex^{2+}) increases solubility in less protic solvents.

B. Small-angle x-ray scattering

1. Influence of metal ion type

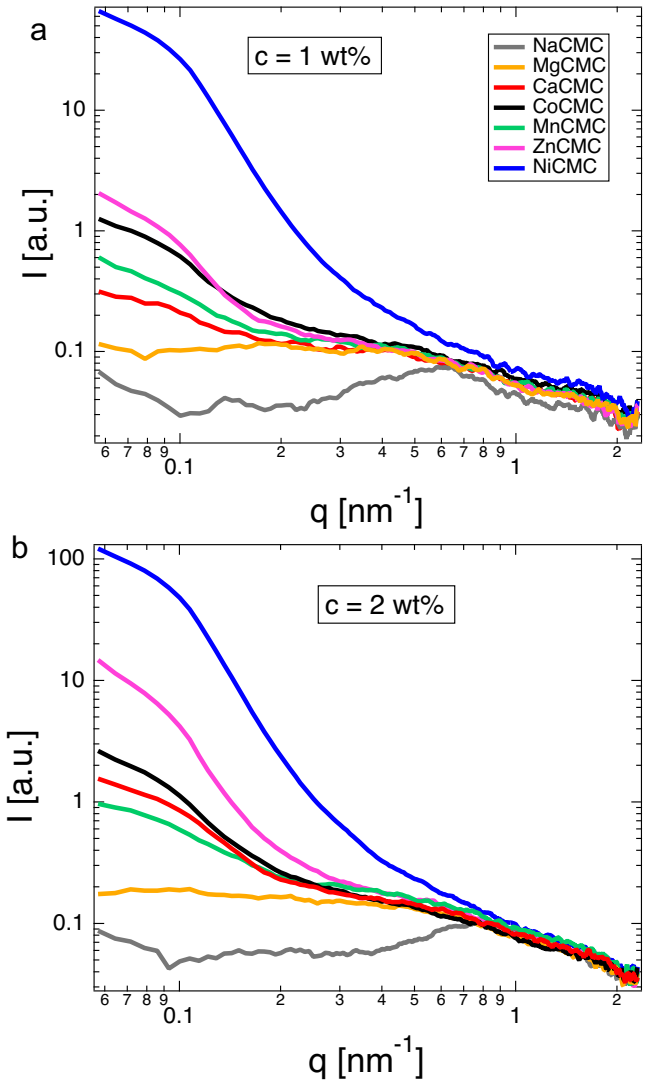

FIG. 5. SAXS profiles of 1 wt% and 2 wt% solutions of NaCMC and divalent metal salts CMC. The counterion is indicated in the legend. Data for sodium and magnesium salts are from ref. [3]. Other data are measured on the in-house instrument.

The SAXS patterns for 1 and 2 wt% NaCMC and divalent metal salt solutions of CMC in DI water are shown in Figure 5. As reported in an earlier study[3], solutions of NaCMC display a correlation peak while those of MgCMC display a broad correlation shoulder, signalling weaker local order. This is consistent with the larger fraction of condensed counterions for the divalent metal salt measured by osmotic pressure, ion-selective potentiometry and conductivity.[2,3,32]

The high/mid$-q$ correlation shoulder in figure 5 is seen to be approximately independent of counterion type. The exception is NiCMC, but this is probably because the contribution of the low$-q$ upturn is still significant in the mid$-q$ region. This suggests that the nature of the metal counterion does not influence the local conformation of CMC, see the calculation of the stretching parameter below. In an earlier study[7] we found the chain dimensions obtained from the overlap concentration for different divalent metal salts of CMC to be independent of counterion type, which is in line with the insensitivity of the correlation length to divalent ion type observed in figure 5.

By contrast, the excess scattering at low-q depends strongly on the identity of the counterion. The nature of the counterions influences the solubility of CMC in water. For example the copper salt of CMC is insoluble and the barium salt is only soluble for high degrees of substitution.[7] Commercial CMC grades such as the one used in this study contain chains with a distribution of degrees of substitution.[64,65] Chains with lower substitution display lower solubility than highly substituted ones.[66] We therefore attribute the stronger low-q upturns observed for the nickel and zinc salts to large aggregates formed by weakly substituted chains, which are not fully soluble in water.

2. Comparison of metal and organic divalent counterions

Figure 6 compares the scattering profiles of NaCMC with those of three divalent salts, MgCMC, HexCMC, and SuxCMC, all in DI water solution without added salts. The comparison between NaCMC and MgCMC has been discussed in detail previously.[3] The transition from peak-like to shoulder-like behavior upon replacing Na^+ with Mg^{2+} is attributed to the lower effective charge density of the MgCMC salt. Conductivity and osmotic pressure data show that for MgCMC, the effective charge of the chain is approximately half that in NaCMC.[3] Although the concentration of free Mg^{2+} ions is only half that of free Na^+ ions, their higher valence leads to a smaller screening length.[67] These effects lead to weaker interchain repulsion for the MgCMC salt and less local ordering on lengthscales of the order of the correlation length, which explains the transition between peak and shoulder behaviour.

For anisotropic counterions Sux^{2+} and Hex^{2+}, a correlation peak is observed for all concentrations studied, indicating stronger electrostatic correlations compared to the magnesium salt. As will be discussed below, this can be explained from the larger fraction of dissociated counterions compared to the magnesium or calcium salts.

3. Correlation length and the stretching parameter

The scaling theory[68,69] predicts the correlation length of a polyelectrolyte solution to be:

$$\xi = \left(\frac{B}{bc}\right)^{1/2} \tag{1}$$

where b is the length of a monomer and c the number concentrations of such monomers. B is the stretching parameter, which quantifies the degree of local folding of the polyelectrolyte. $B = 1$ corresponds to a fully stretched conformation

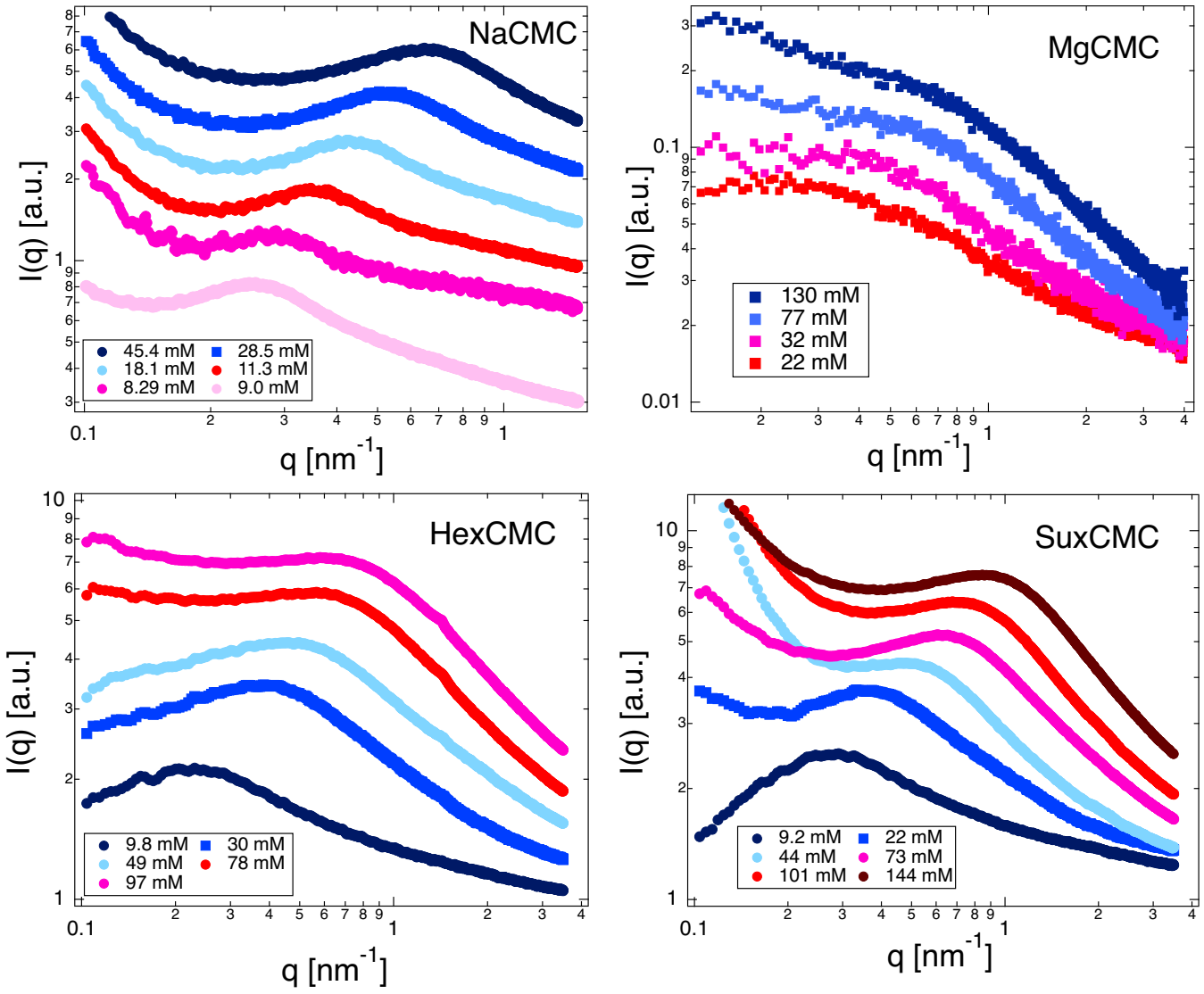

FIG. 6. SAXS profiles for various salts of CMC in arbitrary units, the concentrations are indicated on the legend. Data for the sodium salt are from ref. [62] and data for MgCMC are from ref. [3]. Note that the divalent anisotropic counterion salts display a peak while the spherical Mg salt does not. This is consistent with the lower degree of counterion condensation observed for the organic counterions, see the text for details.

inside the correlation blob. On distances larger than the correlation blob, electrostatics and excluded volume forces are predicted to be screened and chains should adopt random-walk statistics. Experimentally, the correlation length can be calculated from the scattering intensity as:[68,69]

$$\xi = \frac{2\pi}{q^*} \tag{2}$$

where q^* is the wave vector at the local maximum for samples that display a peak or the position of the scattering shoulder for samples which do not display a clear maximum. The position of the shoulder is estimated by fitting power-laws to the high and mid$-q$ regions of the scattering profiles and taking the intercept between these as q^*, see refs. [3,37,70] for details. The values of ξ obtained from Eq. 2 are listed in table II. The simplest approach and the one taken in this work is to fit lines to ($\log q$, $\log I$) the high and mid-q regions and to take the intercept as q^*. The final error for the correlation length was calculated by Gaussian propagation from the regression fitting error for the fit to the spectra.

For NaCMC, the stretching parameter is close to unity, as observed previously for many semiflexible ionic polysaccharides.[3,70] The value $B \simeq 2$ obtained for MgCMC indicates a modest degree of local coiling, similar to that observed in flexible polyelectrolytes with monovalent counterions, such as NaPSS[9,71] or sodium salts of maleic acid copolymers.[72] For the two ditopic organic counterions, the stretching parameter takes an intermediate value of $\simeq 1.5$, indicating a small degree of local folding. Since B is expected to correlate inversely with the effective charge of the chain, the

relation $B_{Na} < B_{Sux} \lesssim B_{Hex} < B_{Mg}$ suggests that the fraction of free counterions follows the opposite order.

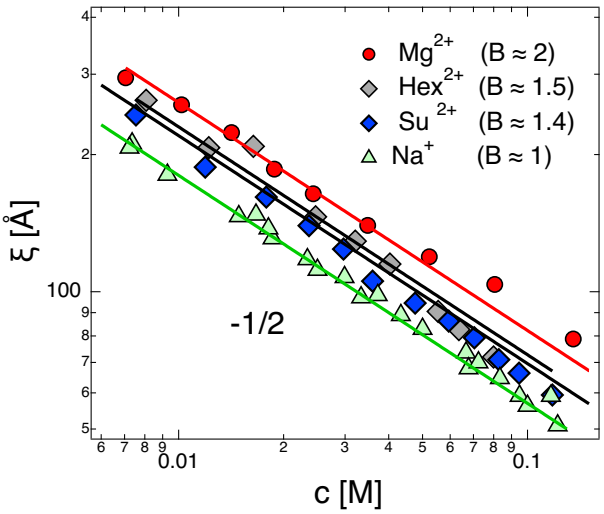

FIG. 7. Correlation length as a function of polymer concentration for the salts in figure 6. The correlation length is calculated from Eq. 1, where q^* is the position of the peak or of the shoulder, see [3] for details. The lines are fits to Eq. 1 with $b = 5.15$ Å and the best-fit B values indicated on the legend. Data for MgCMC are from ref. 3 and for NaCMC are from [62].

4. *Small angle neutron scattering*

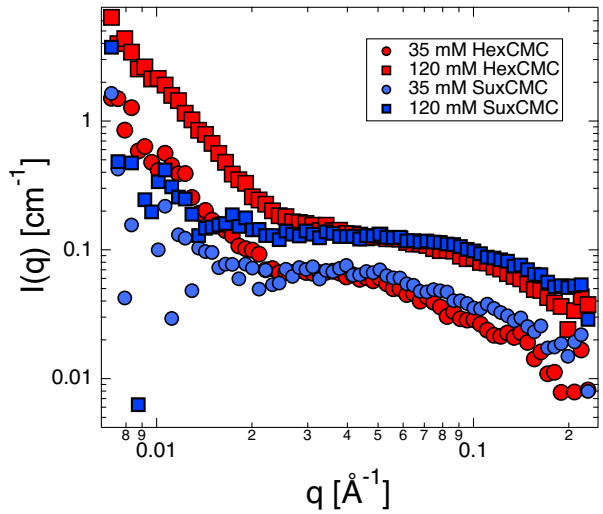

FIG. 8. SANS patterns for solutions of HexCMC and SuxCMC at two different concentrations in D_2O solutions without added salt. In contrast to the SAXS profiles which display a clear peak, the SANS measurements display a correlation shoulder.

Figure 8 shows the small-angle neutron scattering intensity of HexCMC and SuxCMC solutions at 35 and 120 mM in D_2O without added salt. Since the hydrogen-rich counterions scatter more strongly than the backbone, the SANS profiles are dominated by the counterion structure factor. In contrast to the SAXS patterns, which show a clear peak, the SANS profiles display only a broad correlation shoulder, similar to that observed for concentrated TBACMC solutions in Figure 2. We interpret this as evidence that counterion and backbone concentration fluctuations are partially decoupled. Unlike monovalent tetraalkylammonium counterions, for which this decoupling was observed only at high concentrations, HexCMC and SuxCMC show no clear peak even at $c = 35$ mM. The available experimental evidence suggests that decoupling is favoured by counterion hydrophobicity and higher polymer concentration.[37,73] We recently reported that, for TBACMC, this decoupling is suppressed as the dielectric constant of the solvent is decreased.[31] This is intuitive because lowering the solution permittivity promotes counterion condensation. However, in HexCMC and SuxCMC, decoupling in the scattering signal is apparent even though the fraction of condensed counterions remains relatively high, $\simeq 70\%$ for HexCMC.

The low-q upturn is stronger in the SANS measurements than in the SAXS measurements, as observed previously for MgCMC solutions.[3] The origin of this discrepancy is not presently understood, but presumably arises due to differences in contrast between SANS and SAXS.

C. Electrical Conductivity and counterion condensation

The conductivity of the various salts of CMC are listed in table I. Using the model of Colby et al, the specific conductivity of a polyelectrolyte solution can be related to the fraction of monomers with a dissociated counterion as:

$$\Lambda = \left(\lambda_c + \frac{cf\xi^2 e^2 \ln(\xi/D)}{3\pi\eta_s}\right) f \qquad (3)$$

where λ_c is the equivalent limiting ionic conductivity of the counterion, e the electrostatic unit of charge, η_s the solvent viscosity, and D the cross-sectional radius of the chain, taken here to be 7Å .[74]

Equation 3 was used to estimate the fraction of free counterions of CMC salts in previous studies[3,62,75] and compared to other methods.[3] The conductivity estimates for f were $\simeq 30\%$ lower than the more direct measures by potentiometry or osmometry. This is in qualitative agreement with the finding of Katchalsky et al.,[76] who report that charge transport methods yield lower values for f than thermodynamic methods do.[77]

The values of f for the various salts studied are computed using Eq. 3 and the correlation length data in figure 7 and plotted as a function of polymer concentration in figure 9. The magnesium and calcium salts of CMC display a concentration-independent f-value. For the other salts, the fraction of monomers with a dissociated charge increases with increasing concentration. The order of $f_{Na} > f_{Sux} \gtrsim f_{Hex} > f_{Mg} \simeq f_{Ca}$ is consistent with the $B-$values and peak sharpness observed from the SAXS data discussed above, considering that most SAXS data were obtained for $c \gtrsim 0.01$ M.

The independence of f and B from counterion identity for calcium and magnesium CMC suggests that bridging inter-

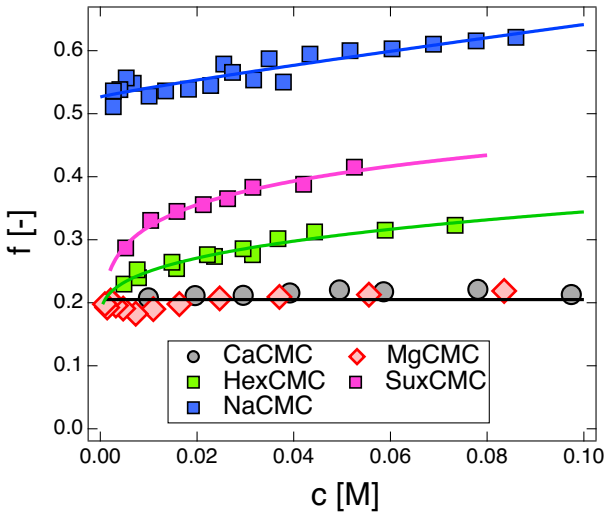

FIG. 9. Fraction of monomers with a dissociated counterions as a function of polymer concentration for five salts of CMC in DI water solutions. Lines are guides to the eye. The f-values are calculated from Eq. 3 using the correlation length values in figure 7.

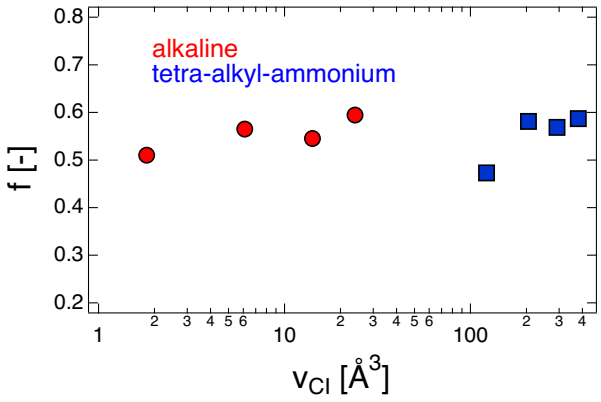

FIG. 10. Fraction of monomers with a dissociated counterion as a function of counterion volume. Red symbols correspond to alkali metals and blue symbols to tetra-alkyl-ammonium ions with alkyl = Me, Et, Pr and Bu. Volumes are calculated as described in ref. [62]. f is obtained by averaging values measured over a concentration range of 0.01-0.15 M for all salts.

actions are absent in this system, in contrast to flexible carboxylate polyelectrolytes, where ion-specific effects can be significant.[78,79] This interpretation is consistent with previous dilute-solution measurements showing that CMC chain dimensions are independent of the divalent metal ion type.[7]

Three possible factors may be considered to explain the larger dissociation observed for the anisotropic ions relative to the metal ones. First, the organic counterions contain an alkane backbone and are therefore more hydrophobic than the metal ions. Second, the organic counterions are anisotropic, whereas the metal ions are approximately spherical. Third, the organic counterions contain two spatially separated 1^+ charges, whereas the metal counterions carry a single 2^+ charge. We consider these possibilities in turn.

Figure 10 plots the fraction of dissociated counterions for CMC with various monovalent counterions as a function of counterion volume. No systematic dependence is observed on either counterion size or hydrophobicity, with the larger alkyl-substituted counterions expected to be the more hydrophobic species. We therefore conclude that hydrophobicity alone cannot account for the enhanced dissociation observed for the organic divalent counterions.

We do not have data on the influence of counterion anisotropy on the fraction of dissociated counterions for monovalent salts of CMC. However, in an earlier study we observed that the stretching parameter was independent of counterion anisotropy,[11] suggesting that f is not strongly affected by counterion shape.

The most plausible explanation for the enhanced counterion dissociation observed in Figure **??** therefore appears to be the ditopic nature of the counterions. As suggested by the earlier theoretical and simulation work discussed in the Introduction, divalent rod-like counterions should behave as a single 2^+ charge when they are far from the polyion backbone, but as two separated monovalent charges when they are close to it. This interpretation is consistent with the concentration dependence of f observed in Figure 11. At low concentrations, where the average distance between counterions and the polyion is large, the ditopic counterions dissociate to a similar extent as Mg^{2+} or Ca^{2+} ions. As the concentration increases, the average counterion–polyion distance decreases, and the ditopic counterions are expected to approach the monovalent-ion limit.

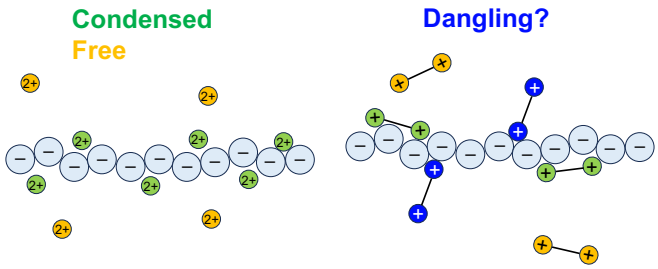

FIG. 11. Schematic representation of the various states of free and condensed divalent counterions. On the left, the two states of the Oosawa-Manning theory are considered. For anisotropic counterions, a different mode of condensation is suggested.

An open question that cannot be fully resolved from the present data is whether separating the 2^+ charge into two 1^+ centers allows the counterions to condense onto the chain without fully neutralising the charge on the backbone. An example of this hypothetical "dangling condensation" state is illustrated schematically in Figure 11. We expect dangling counterions not to contribute significantly to the electrical conductivity of the solution because of their low mobility. Therefore, the f values calculated from Eq. 3 should correspond only to the free counterions. Our SAXS data indirectly support the existence of a dangling counterion state: For concentrations of $\simeq 0.01$ M, the effective charge measured from conductivity is not very different for HexCMC

and Mg/CaCMC but the former show a correlation peak while the alkaline earth metal salts do not. This suggests a higher effective charger for the HexCMC solutions while having a similar concentration of mobile counterions. The existence of such a dangling state may be more decisively tested by dielectric spectroscopy, since the relaxation time of these local dipoles should be much shorter than that of the intermediate-frequency counterion-polarisation relaxation.

IV. CONCLUSIONS

We have studied the solution behaviour of CMC with divalent counterions that differ in charge distribution, comparing small, spherical metal ions with ditopic organic ions in which the two positive charges are spatially separated by a distance of the order of the Bjerrum length. The results show that the nature of the divalent counterion has a clear effect on both charge transport and structure, which is not observed for different monovalent counterions. At comparable concentrations, CMC with anisotropic counterions displays a higher fraction of dissociated counterions than the corresponding divalent metal salts. This difference is small at lower concentrations but becomes pronounced in the semidilute and concentrated regimes.

The scattering data are consistent with the conductivity results. Solutions containing the ditopic counterions exhibit a distinct correlation peak (similar to that of CMC with monovalent counterions), whereas those containing divalent metal ions show only a broad correlation shoulder. This indicates that the ditopic ions give rise to stronger electrostatic correlations and a higher degree of local order, presumably due to their greater dissociation. Analysis of the concentration dependence of the correlation length further shows that the stretching parameter obtained from SAXS follows the same qualitative trend as the effective charge inferred from conductivity. The SAXS and conductivity data therefore provide a consistent picture in which ditopic divalent counterions remain more weakly associated with the backbone than conventional divalent metal ions.

The origin of this enhanced dissociation is not fully understood at present. The available results suggest that neither hydrophobicity nor counterion size alone can account for the observed behaviour. A more plausible explanation is that the spatial separation of charge in the anisotropic ions changes the mode of condensation, allowing partial association without complete local neutralisation of the backbone charge, but this remains a conjecture at present.

No evidence is found of attractive bridging interactions between polymer chains, which have been reported for planar surfaces with rod-like counterions. Our data instead show that counterion anisotropy results in stronger repulsion between chains due to weaker condensation of the counterions.

The findings presented here show that charge topology influences the effective charge and intermolecular correlations of polyelectrolyte solutions. Anisotropic, ditopic counterions therefore provide a useful design parameter for tuning the structure and transport properties of semiflexible polyelectrolytes.

ACKNOWLEDGEMENTS

The authors are grateful to the SPring-8 synchrotron for beamtime (proposal number: 2025B1679) and Dr Noboru Ohta (BL40B2) for his support with the SAXS experiments and data reduction. We thank the ISIS neutron source for beamtime (proposal number: 2690076) and Leide Cavalcanti for conducting the SANS experiments. We also thank Prof. Atsushi Matsumoto and his students Marina Ikeda, Ayaka Ashie and Tokia Maeda, as well as Alan Francisco Mejía and Lingzi Meng for providing laboratory materials, assistance in sample preparation, execution of the experiments and transportation during scattering experiments. The authors also acknowledge the funding bodies that supported this publication, DFG project RI 560/26-1 and JSPS KAKENHI project JP24K01236.

V. APPENDIX: CONDUCTIVITY AND CORRELATION LENGTH DATA

TABLE I. Conductivity (κ), specific conductance (Λ) and fraction of monomers with a dissociated charge (f) of various salts of CMC. Data for MgCMC are from [3].

HxCMC				MgCMC [5.3 mSm^2/mol]			
c [mM]	κ [mS/m]	Λ [Scm^2/mol]	f [-]	c [mM]	κ [mS/m]	Λ [Scm^2/mol]	f [-]
31.5	96.7	30.7	0.276	83.5	171	20.5	0.219
23.6	73.2	31.0	0.273	55.5	114	20.5	0.213
15.8	45.5	28.9	0.254	37.0	76.6	20.7	0.209
7.9	22.0	27.9	0.240	24.7	52.0	21.1	0.207
4.88	13.2	27.0	0.230	16.3	33.3	20.4	0.198
73.4	260	35.4	0.323	11.0	21.7	19.8	0.190
58.9	206	35.0	0.315	7.33	14.1	19.2	0.183
44.3	157	35.4	0.312	4.72	10.0	21.2	0.191
36.7	126	34.3	0.302	3.23	7.3	22.6	0.196
29.5	95.6	32.4	0.286	2.14	5.3	24.7	0.204
22.2	70.0	31.6	0.276	1.42	3.3	23.3	0.192
14.8	45.4	30.6	0.264	0.962	2.4	24.9	0.198
7.62	22.9	30.1	0.252				
SuxCMC				CaCMC [5.95 mSm^2/mol]			
c [mM]	κ [mS/m]	Λ [Scm^2/mol]	f [-]	c [mM]	κ [mS/m]	Λ [Scm^2/mol]	f [-]
52.6	166	31.6	0.415	97.4	196	20.1	0.213
42.0	123	29.3	0.388	78.1	169	21.6	0.221
31.6	94	29.8	0.383	58.6	127	21.7	0.217
26.3	74.3	28.2	0.365	49.5	111	22.4	0.220
21.3	59.1	27.8	0.356	39.2	87	22.2	0.216
15.9	43.4	27.4	0.345	29.6	65.5	22.2	0.212
10.4	27.9	26.8	0.331	19.6	44.8	22.9	0.211
5.26	12.0	22.8	0.287	9.94	23.4	23.5	0.208

BIBLIOGRAPHY

[1] C. G. Lopez, A. Matsumoto, and A. Q. Shen, "Dilute polyelectrolyte solutions: recent progress and open questions," Soft Matter **20**, 2635–2687 (2024).

[2] M. Rinaudo and M. Milas, "Interaction of monovalent and divalent counterions with some carboxylic polysaccharides," J. Polym. Sci., Polym. Chem. Ed. **12**, 2073–2081 (1974).

TABLE II. Correlation length ξ for SuxCMC and HexCMC solutions. The uncertainties were calculated by error progation fro the fitting parameters for the fits around the peaks or shoulders.

SuxCMC		HexCMC	
c [M]	ξ [Å]	c [M]	ξ [Å]
0.00755	244 ± 10	0.00807	263 ± 8
0.0119	188 ± 2	0.0122	207 ± 4
0.0178	161 ± 2	0.0164	208 ± 4
0.0236	140 ± 2	0.0247	146 ± 1
0.0297	124.0 ± 0.9	0.0321	129.1 ± 1.0
0.0360	105.5 ± 0.4	0.0403	115.1 ± 0.6
0.0476	94.5 ± 0.3	0.0554	90.5 ± 0.3
0.0595	86.2 ± 0.2	0.0636	82.6 ± 0.3
0.0704	79.3 ± 0.3	0.0799	71.9 ± 0.2
0.0827	71.0 ± 0.3		
0.0945	66.3 ± 0.2		
0.118	59.4 ± 0.2		

[3] E. A. GharehTapeh, T. Watanabe, F. Horkay, C. Hou, C. Lopez, and M. Hohenschutz, "Counterion condensation, ion pairing and scattering properties of carboxymethyl cellulose with mono- and divalent ions." Cellulose, accepted (2026).

[4] H. Magdelenat, P. Turr, P. Tivant, M. Chemla, R. Menez, and M. Drifford, "The effect of counter-ion substitution on the transport properties of polyelectrolyte solutions," Biopolymers: Original Research on Biomolecules **18**, 187–201 (1979).

[5] Y. Zhang, J. F. Douglas, B. D. Ermi, and E. J. Amis, "Influence of counterion valency on the scattering properties of highly charged polyelectrolyte solutions," J. Chem. Phys. **114**, 3299–3313 (2001).

[6] E. Dubois and F. Boué, "Conformation of poly (styrenesulfonate) polyions in the presence of multivalent ions: small-angle neutron scattering experiments," Macromolecules **34**, 3684–3697 (2001).

[7] C. G. Lopez and W. Richtering, "Influence of divalent counterions on the solution rheology and supramolecular aggregation of carboxymethyl cellulose," Cellulose **26**, 1517–1534 (2019).

[8] M. Jacobs, C. G. Lopez, and A. V. Dobrynin, "Quantifying the effect of multivalent ions in polyelectrolyte solutions," Macromolecules **54**, 9577–9586 (2021).

[9] C. G. Lopez, F. Horkay, R. Schweins, and W. Richtering, "Solution properties of polyelectrolytes with divalent counterions," Macromolecules **54**, 10583–10593 (2021).

[10] T. Ono, M. Ohta, and K. Sada, "Ionic polymers act as polyelectrolytes in nonpolar media," ACS Macro Lett. **1**, 1270–1273 (2012), pMID: 35607154, https://doi.org/10.1021/mz3002879.

[11] C. Hou, W. Richtering, T. Watanabe, K. Leonhard, M. Papusha, and C. G. Lopez, "Solutions of carboxymethylcellulose with organic counterions (i): The influence of counterion properties on the polymer structure and solubility," Macromolecules **58**, 7489–7499 (2025).

[12] J. Szymczak, P. Holyk, and P. Ander, "Electrical conductivity of aqueous solutions of monovalent salts of polystyrenesulfonate," J. Phys. Chem. **79**, 269–272 (1975).

[13] S. Kondou, Y. Sakashita, A. Morinaga, Y. Katayama, K. Dokko, M. Watanabe, and K. Ueno, "Concentrated nonaqueous polyelectrolyte solutions: high na-ion transference number and surface-tethered polyanion layer for sodium-metal batteries," ACS Applied Materials & Interfaces **15**, 11741–11755 (2023).

[14] T. Okubo, "Surface tension of synthetic polyelectrolyte solutions at the air-water interface," Journal of colloid and interface science **125**, 386–398 (1988).

[15] F. Oosawa, *Polyelectrolytes* (Marcel Dekker, Inc. New York, 1971).

[16] R. Zana, C. Tondre, M. Rinaudo, and M. Milas, "Étude ultrasonore de la fixation sur site des ions alcalins sur des carboxymethylcelluloses de densité de charge variable," Journal de Chimie Physique **68**, 1258–1266 (1971).

[17] C. Tondre and R. Zana, "Apparent molal volumes of polyelectrolytes in aqueous solutions," The Journal of Physical Chemistry **76**, 3451–3459 (1972).

[18] C. Tondre and R. Zana, "Ultrasonic absorption and density studies of counter-ion site binding in aqueous solutions of polyelectrolytes," in *Polyelectrolytes: Papers Initiated by a NATO Advanced Study Institute on Charged and Reactive Polymers held in France, June 1972* (Springer, 1974) pp. 323–338.

[19] R. Zana and C. Tondre, "Ultrasonic studies of polyion polyelectrolytes solutions," Chemical and Biological Applications of Relaxation Spectrometry: Proceedings of the NATO Advanced Study Institute Held at the University of Salford, Salford, England, 29 August–12 September, 1974 **18**, 333 (1975).

[20] J. Komiyama, M. Ando, Y. Takeda, and T. Iuma, "Dilatometric study of monovalent counter-ion association with carboxylates," European Polymer Journal **12**, 201–207 (1976).

[21] M. Satoh, E. Yoda, and J. Komiyama, "Effects of hydrophobic hydration on counterion binding of polycations," Macromolecules **24**, 1123–1127 (1991).

[22] M. Satoh, T. Kawashima, and J. Komiyama, "Competitive counterion binding and dehydration of polyelectrolytes in aqueous solutions," Polymer **32**, 892–896 (1991).

[23] S. Koda, Y. Sugi, T. Sakurai, T. Matsuoka, and H. Nomura, "Study on segmental motion and ion binding in polyelectrolyte solutions by ultrasonic spectroscopy," Journal of solution chemistry **33**, 747–760 (2004).

[24] Y. Marcus and G. Hefter, "Ion pairing," Chemical reviews **106**, 4585–4621 (2006).

[25] Y. Marcus, "Electrostriction in electrolyte solutions," Chemical Reviews **111**, 2761–2783 (2011).

[26] U. P. Strauss and P. D. Ross, "Counterion binding by polyelectrolytes. iv. membrane equilibrium studies of the binding of univalent cations by long-chain polyphosphates," Journal of the American Chemical Society **81**, 5299–5302 (1959).

[27] U. P. Strauss and Y. P. Leung, "Volume changes as a criterion for site binding of counterions by polyelectrolytes," Journal of the American Chemical Society **87**, 1476–1480 (1965).

[28] R. H. Colby, D. C. Boris, W. E. Krause, and J. S. Tan, "Polyelectrolyte conductivity," J. Polym. Sci. B: Polym. Phys. **35**, 2951–2960 (1997).

[29] Y. Marcus, "Tetraalkylammonium ions in aqueous and non-aqueous solutions," Journal of Solution Chemistry **37**, 1071–1098 (2008).

[30] M. Rinaudo, J. Mazet, and M. Milas, "Propriétés thermodynamiques des polyanions à densité de charge variable," CR Acad. Sci. , 1401–1404 (1973).

[31] A. Gulati, L. Meng, C. Hou, T. Watanabe, and C. G. Lopez, "Solution structure and counterion condensation of carboxymethyl cellulose in organic solvents." Submitted to ACS Applied Polymer Materials (2026).

[32] M. Rinaudo, "Polyelektrolyteigenschaften von carboxymethylcellulose in wäßriger lösung-einfluß der ladungsdichte1," (1973).

[33] M. Rinaudo and M. Milas, "Propriétés électrochimiques des polyélectrolytes à densité de charge élevée," Journal de Chimie Physique **66**, 1489–1496 (1969).

[34] C. Yomota, S. Okada, K. Mochida, and M. Nakagaki, "The molal osmotic coefficients and counterion activity coefficients of arabate with various counterions," Chemical and pharmaceutical bulletin **32**, 3793–3802 (1984).

[35] I. Satake, M. Fukuda, T. Ohta, K. Nakamura, N. Fujita, A. Yamauchi, and H. Kimizuka, "Interactions of counterions with dextran sulfate in aqueous solutions," J. Polym. Sci. Polym. Phys. Ed. **10**, 2343–2354 (1972).

[36] H. T. Masakatsu Yonese and H. Kishimoto, "Practical osmotic coefficients of chondroitin sulfate a and c salts with various counterions," Journal of the Chemical Society of Japan (Chemistry and Industrial Chemistry) **1978**, 108–112 (1978).

[37] A. Gulati, J. F. Douglas, O. Matsarskaia, and C. G. Lopez, "Influence of counterion type on the scattering of a semiflexible polyelectrolyte," Soft matter **20**, 8610–8620 (2024).

[38] A. Chremos and J. F. Douglas, "Polyelectrolyte association and solvation," The Journal of chemical physics **149** (2018).

[39] A. Chremos and J. F. Douglas, "The influence of polymer and ion solvation on the conformational properties of flexible polyelectrolytes," Gels **4**, 20 (2018).

[40] A. Chremos and F. Horkay, "Disappearance of the polyelectrolyte peak in salt-free solutions," Physical Review E **102**, 012611 (2020).

[41] S. Ghosh and A. Kundagrami, "Effect of counterion size on polyelectrolyte conformations and thermodynamics," The Journal of Chemical Physics **160** (2024).

[42] A. Tagliabue and M. Mella, "The role of counterion size in defining star-shaped polyelectrolytes thermodynamics, conformations, and ion dynamics," Journal of Polymer Science **63**, 3005–3022 (2025).

[43] Y. W. Kim, J. Yi, and P. Pincus, "Attractions between like-charged surfaces with dumbbell-shaped counterions," Physical review letters **101**, 208305 (2008).

[44] J. Urbanija, K. Bohinc, A. Bellen, S. Maset, A. Iglič, V. Kralj-Iglič, and P. Sunil Kumar, "Attraction between negatively charged surfaces mediated by spherical counterions with quadrupolar charge distribution," The Journal of chemical physics **129** (2008).

[45] S. Maset, J. Reščič, S. May, J. I. Pavlič, and K. Bohinc, "Attraction between like-charged surfaces induced by orientational ordering of divalent rigid rod-like counterions: theory and simulations," Journal of Physics A: Mathematical and Theoretical **42**, 105401 (2009).

[46] J. M. Grime, M. O. Khan, and K. Bohinc, "Interaction between charged surfaces mediated by rodlike counterions: the influence of discrete charge distribution in the solution and on the surfaces," Langmuir **26**, 6343–6349 (2010).

[47] M. Cha, S. Ro, and Y. W. Kim, "Rodlike counterions near charged cylinders: counterion condensation and intercylinder interaction," Physical Review Letters **121**, 058001 (2018).

[48] M. Cha, S. Ro, and Y. W. Kim, "Condensation of rodlike counterions on a charged cylinder," Journal of the Korean Physical Society **77**, 811–818 (2020).

[49] D. A. Rytand, "The use of hexamethonium in arterial hypertension," California Medicine **80**, 375 (1954).

[50] A. Campbell and E. Robertson, "Treatment of severe hypertension with hexamethonium bromide," British Medical Journal **2**, 804 (1950).

[51] C. B. Rich and W. H. Holubitsky, "Hexamethonium in hypertension," Canadian Medical Association Journal **68**, 342 (1953).

[52] V. I. Skok, "Ganglion blockers," in *Mechanisms of Drug Action: Volume 1*, edited by G. N. Woodruff (Springer, 1986) pp. 97–129.

[53] W. Paton, "Hexamethonium," British Journal of Clinical Pharmacology **13**, 7 (1982).

[54] G. Giordano, J. Nagy, and E. Derouane, "Zeolite synthesis in presence of hexamethonium ions," Journal of Molecular Catalysis A: Chemical **305**, 34–39 (2009).

[55] N. Bats, L. Rouleau, J.-L. Paillaud, P. Caullet, Y. Mathieu, and S. Lacombe, "Recent developments in the use of hexamethonium salts as structure directing agents in zeolite synthesis," Studies in Surface Science and Catalysis **154**, 283–288 (2004).

[56] X. Liu, U. Ravon, and A. Tuel, "Synthesis of all-silica zeolites from highly concentrated gels containing hexamethonium cations," Microporous and mesoporous materials **156**, 257–261 (2012).

[57] L. Piotrovskiy, E. Litasova, M. Dumpis, D. Nikolaev, E. Yakovleva, O. Dravolina, and A. Y. Bespalov, "Enhanced brain penetration of hexamethonium in complexes with derivatives of fullerene c60," in *Doklady Biochemistry and Biophysics*, Vol. 468 (Springer, 2016) pp. 173–175.

[58] F.-Y. Hsieh, A. Zhilenkov, I. Voronov, E. Khakina, D. Mischenko, P. A. Troshin, and S.-h. Hsu, "Water-soluble fullerene derivatives as brain medicine: surface chemistry determines if they are neuroprotective and antitumor," ACS applied materials & interfaces **9**, 11482–11492 (2017).

[59] M. A. F. de Godoy, D. Accorsi-Mendonça, and A. M. de Oliveira, "Inhibitory effects of atropine and hexamethonium on the angiotensin ii-induced contractions of rat anococcygeus smooth muscles," Naunyn-Schmiedeberg's archives of pharmacology **367**, 176–182 (2003).

[60] E. Karavaev, I. Y. Popova, and V. Kichigina, "The nicotinic receptor blocker hexamethonium alters neuronal responses to glutamate in the medial septal area of the brain of the ground squirrel in vitro," Neuroscience and Behavioral Physiology **38**, 297–307 (2008).

[61] P. Li, J.-X. Gong, W. Sun, B. Zhou, and X.-Q. Kong, "Hexamethonium attenuates sympathetic activity and blood pressure in spontaneously hypertensive rats," Molecular Medicine Reports **12**, 7116–7122 (2015).

[62] C. Hou, T. Watanabe, C. G. Lopez, and W. Richtering, "Structure and rheology of carboxymethylcellulose in polar solvent mixtures," Carbohydrate Polymers **347**, 122287 (2025).

[63] The exception is $ZnCl_2$: addition of a large excess zinc ions does not precipitate the solution. As the dialysis proceeds the polymer precipitates and then redissolves, indicating the existence of a re-entrant phase. Such behaviour has been observed for other polyelectrolytes in the presence of trivalent and tetra-valent ions.[1].

[64] K. A. Oudhoff, F. A. Buijtenhuijs, P. H. Wijnen, P. J. Schoenmakers, and W. T. Kok, "Determination of the degree of substitution and its distribution of carboxymethylcelluloses by capillary zone electrophoresis," Carbohydrate research **339**, 1917–1924 (2004).

[65] M. Shakun, T. Heinze, and W. Radke, "Determination of the ds distribution of non-degraded sodium carboxymethyl cellulose by gradient chromatography," Carbohydrate polymers **98**, 943–950 (2013).

[66] K. Kamide, K. Okajima, K. Kowsaka, T. Matsui, S. Nomura, and K. Hikichi, "Effect of the distribution of substitution of the sodium salt of carboxymethylcellulose on its absorbency toward aqueous liquid," Polymer journal **17**, 909–918 (1985).

[67] The screening length $\kappa^{-1} \simeq 1/\sqrt{4\pi l_B \frac{1}{2}\sum_i c_i Z_i^2}$, where κ^{-1} is the Debye screening length, l_B the Bjerrum length and c_i and Z_i are the number concentration and valence of the ith ion.

[68] A. V. Dobrynin, R. H. Colby, and M. Rubinstein, "Scaling theory of polyelectrolyte solutions," Macromolecules **28**, 1859–1871 (1995).

[69] A. V. Dobrynin and M. Rubinstein, "Theory of polyelectrolytes in solutions and at surfaces," Prog. Polym. Sci. **30**, 1049–1118 (2005).

[70] K. Salamon, D. Aumiler, G. Pabst, and T. Vuletic, "Probing the mesh formed by the semirigid polyelectrolytes," Macromolecules **46**, 1107–1118 (2013).

[71] A. Han and R. H. Colby, "Rheology of entangled polyelectrolyte solutions," Macromolecules **54**, 1375–1387 (2021).

[72] E. Di Cola, N. Plucktaveesak, T. Waigh, R. Colby, J. Tan, W. Pyckhout-Hintzen, and R. Heenan, "Structure and dynamics in aqueous solutions of amphiphilic sodium maleate-containing alternating copolymers," Macromolecules **37**, 8457–8465 (2004).

[73] J. Combet, F. Isel, M. Rawiso, and F. Boué, "Scattering functions of flexible polyelectrolytes in the presence of mixed valence counterions: condensation and scaling," Macromolecules **38**, 7456–7469 (2005).

[74] C. G. Lopez, S. E. Rogers, R. H. Colby, P. Graham, and J. T. Cabral, "Structure of sodium carboxymethyl cellulose aqueous solutions: A sans and rheology study," J. Polym. Sci. B: Polym. Phys. **53**, 492–501 (2015).

[75] D. Ray, R. De, and B. Das, "Thermodynamic, transport and frictional properties in semidilute aqueous sodium carboxymethylcellulose solution," J. Chem. Thermodyn. **101**, 227–235 (2016).

[76] K. O. Katchalsky A, Alexandrowicz Z, "Chemical physics of ionic solutions: a selection of invited papers and discussions presented at an international symposium of the electrochemical society in toronto, canada, may 4-6, 1964," (No Title) (1966).

[77] One possible reason is that Eq. 3 assumes that the diffusion of a free counterion is the same as that of that ion in a simple electrolyte solution in the infinite dilution limit. Experiments show that counterion diffusion is slowed down by the polyion.[80–84].

[78] A. Glisman, S. Mantha, D. Yu, E. P. Wasserman, S. Backer, and Z.-G. Wang, "Multivalent ion-mediated polyelectrolyte association and structure," Macromolecules **57**, 1941–1949 (2024).

[79] S. Mantha, A. Glisman, D. Yu, E. P. Wasserman, S. Backer, and Z.-G. Wang, "Adsorption isotherm and mechanism of ca2+ binding to polyelectrolyte," Langmuir **40**, 6212–6219 (2024).

[80] W. Lubas and P. Ander, "Sodium ion diffusion coefficients in aqueous salt-free polyelectrolyte solutions," Macromolecules **13**, 318–321 (1980).

[81] P. Ander and W. Lubas, "Sodium ion diffusion in aqueous salt-free heparin solutions," Macromolecules **14**, 1058–1061 (1981).

[82] P. Ander and M. Kardan, "Interactions of sodium ions with polyelectrolytes of constant charge density," Macromolecules **17**, 2436–2441 (1984).

[83] C. T. Henningson, D. Karluk, and P. Ander, "Comparison of sodium ion interactions with sodium salts of (carboxymethyl) cellulose and vinylic polyelectrolytes of varying charge density by diffusion," Macromolecules **20**, 1286–1291 (1987).

[84] F. Schipper, K. Kassapidou, and J. Leyte, "Polyelectrolyte effects on counterion self-diffusion," Journal of Physics: Condensed Matter **8**, 9301–9308 (1996).